Journal of Cell Science 111, 2269-2282 (1998)
Printed in Great Britain © The Company of Biologists Limited 1998
JCS4558



# The path of transcripts from extra-nucleolar synthetic sites to nuclear pores: transcripts in transit are concentrated in discrete structures containing SR proteins

**F. J. Iborra, D. A. Jackson and P. R. Cook***

The Sir William Dunn School of Pathology, University of Oxford, South Parks Road, Oxford OX1 3RE, UK
*Author for correspondence (e-mail: peter.cook@path.ox.ac.uk)

*Accepted 19 May; published on WWW 15 July 1998*

## SUMMARY

**The route taken by transcripts from synthetic sites in the nucleus to the cytoplasm has been under scrutiny for years, but details of the pathway remain obscure. A new high-resolution method for mapping the pathway is described; HeLa cells are grown in Br-U so that the analogue is incorporated into RNA and exported to the cytoplasm, before Br-RNA is localized by immuno-electron microscopy. After exposure to low concentrations of Br-U for short periods, cells grow normally. Br-RNA is first found in several thousand extra-nucleolar transcription sites or factories (diameter 50-80 nm), before appearing in several hundred new downstream sites (diameter 50-80 nm) each minute; subsequently, progressively more downstream sites become labelled. These sites can be isolated on sucrose gradients as large nuclear ribonucleoprotein particles of ~200 S. Later, Br-RNA is seen docked ~200 nm away from ~20% nuclear pores, before exiting to the cytoplasm. Individual downstream sites are unlikely to contain individual transcripts; rather, results are consistent with groups of transcripts being shipped together from synthetic sites to pores. A subset of SR proteins are excellent markers of this pathway; this subset is concentrated in tens of thousands of sites, which include transcription, downstream and docking sites. Growth in high concentrations of Br-U for long periods is toxic, and Br-RNA accumulates just inside nuclear pores.**

Key words: Biotin-CTP, Bromouridine, Immunogold labelling, Stereology

## INTRODUCTION

Nascent transcripts first appear within the nucleoplasm in perichromatin fibrils (e.g. Fakan et al., 1976; Fakan, 1994), but then the route that those transcripts take to the cytoplasm is obscure (for reviews, see Spector, 1993; Izaurralde and Mattaj, 1995; Corbett and Silver, 1997; Daneholt, 1997; Nigg, 1997). Various factors make analysis difficult. First, some primary transcripts are completely degraded, and splicing shortens many of the remainder; as a result, ~5% hnRNA reaches the cytoplasm as mRNA (Ross, 1995; Jacobson and Peltz, 1996). Second, individual transcripts are packaged into ribonucleoprotein particles that have dimensions below the resolution of the light microscope (i.e. ~200 nm; reviewed by Sharp, 1994; Sperling et al., 1997). Third, transport is rapid; for example, hnRNP particles could travel many hundreds of nanometers in a few seconds by diffusion, or if powered by one of the known cellular motors (e.g. the actin-myosin I system). Fourth, few high-resolution techniques are available to label nascent transcripts so that their path can be mapped accurately. Thus, autoradiographic grains may lie >100 nm from a $^{3}H$ source in RNA, and interpretations of experiments involving fluorescence in situ hybridization are often based upon assumptions concerning rates and order of splicing, and that nuclear structure has been adequately preserved during the harsh conditions used during annealing.

Recently, high-resolution methods have been developed to visualize sites containing nascent RNA. In one approach, cells are permeabilized and allowed to extend nascent transcripts in Br-UTP or biotin-CTP, while a variant involves microinjecting Br-UTP directly into living cells; then, sites containing Br- or bio-RNA are immunolabelled with fluorescent antibodies or gold particles (Jackson et al., 1993; Wansink et al., 1993; Iborra et al., 1996). In a second approach, living cells are grown in Br-U before sites containing incorporated analogues are immunolabelled with gold particles (Hozák et al., 1994). A logical extension of this second approach is to grow cells in Br-U, and then follow newly made Br-RNA to the cytoplasm. However, some reports suggest that Br-U is incorporated poorly into RNA, and that the presence of bromine in RNA inhibits transport and/or processing. For example, microinjection of high concentrations of Br-UTP into living cells is toxic and prevents transport to the cytoplasm (Fay et al., 1997), while complete substitution of U by Br-U inhibits splicing and translation in vitro (Sierakowska et al., 1989; Wansink et al., 1994; Schmittgen et al., 1994). Despite these difficulties, we reasoned that Br-RNA might be made and transported properly if it contained only a few Br-U residues.

Therefore, we grew HeLa cells in a range of different Br-U concentrations, and monitored both incorporation and transport. We find that Br-U is incorporated efficiently by nucleoplasmic polymerases at all concentrations tested. Moreover, cells grow normally in moderate concentrations of Br-U, and the resulting Br-RNA is transported to the cytoplasm.

Using this high-resolution method, we have mapped the pathway to the cytoplasm. Initially Br-RNA is found only in several thousand extra-nucleolar transcription sites. Then Br-RNA appears in several hundred new downstream sites each minute. These sites contain a subset of SR antigens, a group of splicing factors that contain serine- and arginine-rich carboxy-terminal domains (Zahler et al., 1992; reviewed by Kramer, 1996). They can also be isolated on sucrose gradients as large nuclear ribonucleoprotein particles of ~200 S (Sperling et al., 1997). Later, Br-RNA docks just inside nuclear pores, before exiting to the cytoplasm. It is unlikely that individual transcripts are detected in transit between transcription sites and pores; results are consistent with groups of transcripts being shipped together.

## MATERIALS AND METHODS

### Cell growth, encapsulation, lysis and buffers

HeLa cells in suspension were grown, encapsulated in agarose, and lysed with saponin (100 μg/ml; 3 minutes; Sigma) in a 'physiological' buffer (PB; Jackson et al., 1993). PB is 100 mM potassium acetate, 30 mM KCl, 10 mM $Na_2HPO_4$, 1 mM $MgCl_2$, 1 mM $Na_2ATP$ (Sigma Grade I), 1 mM dithiothreitol, and 0.2 mM phenylmethylsulphonyl fluoride (pH 7.4). As the acidity of ATP batches can vary, 100 mM $KH_2PO_4$ (usually ≤1/100th volume) is sometimes added to adjust the pH. PB* is PB plus human placental ribonuclease inhibitor (10 units/ml; Amersham). Hypotonic PB is 1 volume of PB plus 2 volumes of distilled water, and 1 mM dithiothreitol, 0.5 mM phenylmethylsulphonyl fluoride, and 5 units/ml ribonuclease inhibitor. Buffers used immediately before, during, and after, lysis were ice-cold, unless stated otherwise.

The effects of Br-U on growth were measured after plating $0.25\times10^6$ cells in 25 $cm^2$ flasks in 5 ml Dulbecco's modification of MEM. One day after plating, cells were exposed to Br-U, washed in medium, regrown for 1 hour in 50 μM uridine, rewashed, and regrown; fresh medium was added every two days. Numbers of live (i.e. spread) cells in random fields were counted daily from 1 day before to 5 days after exposure using a phase-contrast microscope. Monolayers were also used for autoradiography (see Table 6). Cells were grown for 1 hour in [5-$^3$H]C (10 μCi/ml; 23 Ci/mmol; DuPont) ± aphidicolin (5 μg/ml; added 15 minutes before the beginning of the pulse) ± 2.5 mM Br-U, and some were washed and regrown for 23 hours in the absence of any additives other than 0.5 mM U. After fixation and acid extraction, autoradiographs were prepared using K5 emulsion (Ilford; Lasnitzki, 1992), exposed for 24 hours, and the numbers of silver grains over different compartments counted.

### Immunogold labelling

Cells were grown in Br-U, prefixed (10 minutes; 0°C) with 4% paraformaldehyde in 250 mM Hepes (pH 7.4), fixed (50 minutes; 20°C) with 8% paraformaldehyde in the same buffer, partially dehydrated in ice-cold ethanol, embedded in LR White (polymerization by heat for 4 hours at 50°C, or uv-irradiation for 4 days at –20°C; London Resin Company), and Br-RNA on ultrathin sections on nickel grids indirectly immunolabelled using Protein A absorbed on to gold particles. Nonspecific binding was blocked by preincubation (30 minutes) in PBS (pH 8.2) with 0.1% Tween-20 and 1% BSA. Next, sections were incubated (2 hours) with a monoclonal anti-bromodeoxyuridine antibody (Boehringer; 10 μg/ml in PBS with Tween and BSA) that reacts with Br-RNA, washed in PBS (pH 8.2), incubated (1 hour) with rabbit anti-mouse IgG (1:50 dilution; Jackson labs) in PBS plus Tween and BSA, rewashed, incubated (1 hour) with Protein A absorbed on to 5 or 9 nm gold particles (1:100 dilution spun immediately before use to remove aggregates; prepared as described by Griffiths, 1993) in PBS with BSA, rewashed, and fixed with 2.5% glutaraldehyde. Then sections were washed with water, dried, and contrasted with a saturated solution of uranyl acetate in 70% ethanol. Sections were observed in a Zeiss 912 Omega electron microscope, before digital images were collected and analyzed (Iborra et al., 1996).

Sites containing both Br- and biotin-RNA (bio-RNA) were analyzed as follows, using the general procedures described above. Cells were encapsulated ($10^7$/ml), grown (2 hours), regrown in Br-U, washed 2× in PBS, 1× in PB, lysed, and washed 2× in PB. Packed beads in the pellet (250 μl) were immediately added to transcription reactions (500 μl) which contained PB* plus 100 μM ATP, biotin-CTP (bio-CTP; Gibco-BRL), GTP and UTP, and 0.4 mM $MgCl_2$ (PB already contains 1 mM $MgCl_2$). After 15 minutes at 33°C, samples were fixed and sectioned. Bio-RNA was labelled using a goat anti-biotin antibody (5 μg/ml; Jackson Laboratories) and then a rabbit anti-goat IgG conjugated with 5 nm gold particles (1:50 dilution; BioCell). Samples were fixed (1% glutaraldehyde; 15 minutes), and incubated with 50 mM $NH_4Cl$ (1 hour) and 10% foetal calf serum (30 minutes; Griffiths, 1993), before Br-RNA was labelled with 9 nm particles.

For preembedment immunolabelling, cells were encapsulated, grown in Br-U, extracted with 0.25% Triton and 2 M NaCl, immunolabelled using Protein A conjugated with 5 nm gold particles rather than 1 nm particles, embedded and imaged, all as described by Iborra et al. (1996). Extraction swells cells, increasing nucleoplasmic volume from 400 to 550 $\mu m^3$ (Iborra et al., 1996).

For Fig. 5, phosphorylated SR antigens were detected using a 1/100 dilution of the supernatant produced by cell line m104 (ATCC CRL-2067; Roth et al., 1990) and a secondary goat antibody against mouse IgG conjugated with 5 or 9 nm gold particles (BioCell; 1/100 dilution). When double-labelling, bio-RNA or Br-RNA were labelled as above, before labelling SR proteins. For Fig. 5D, particles isolated on sucrose gradients (see below) were adsorbed (5 minutes; 20°C) on to carbon-coated nickel grids, washed with water, and negatively stained with 1% uranyl acetate (15 seconds). For Fig. 5E, adsorbed particles were fixed in 4% paraformaldehyde in PBS (30 minutes), immunolabelled (as above), before washing with water and staining with uranyl acetate (as above). For Fig. 5F, samples were treated as for Fig. 5E except that the primary antibody was the monoclonal anti-bromodeoxyuridine antibody. Nuclear pores and Br-RNA were colabelled in Fig. 6B using mouse anti-nucleoporin p62 (clone 53; Transduction Labs) and then goat anti-mouse IgG conjugated with gold particles (5 nm), followed by fixation with glutaraldehyde, incubation successively with the anti-bromodeoxyuridine antibody, rabbit anti-mouse IgG, and Protein A absorbed on 9 nm gold particles.

### Stereology

Stereological analysis followed established procedures (Williams, 1977). (1) Collection of 50 images like those in Fig. 1. (2) Measurement (using 'SIS' software) of: (i) major, 2*x*, and minor, 2*y*, (orthogonal) axes of each cluster, (ii) area of each cluster, (iii) numbers of clusters or particles in a compartment (e.g. nucleoplasm), and (iv) area of compartment. (3) Calculation (using 'Excel' and algorithms kindly supplied by J. Renau-Piqueras) of: (i) cluster diameter, D, from $D = 2\sqrt{(xy)}$, (ii) mean cluster diameter, $D_m$, of the Gaussian population using Fullman's formula, (iii) shape, β, and distribution constant, K, (iv) mean area, a, and volume, v, of clusters from $v = \beta a^{3/2}$, and (v) finally the number of clusters/unit volume, $N_v$, using the expression of DeHoff and Rhines. Values for major/minor nuclear/nucleolar axes, and mean diameters and volumes, were taken

from Iborra et al. (1996). The volume of the cytoplasm was determined from the nuclear volume and volume fraction ($V_v$), where $V_v$ = $volume_{nucleus}/volume_{cytoplasm}$ = $area_{nucleus}/area_{cytoplasm}$. In all cases (i) sample numbers analysed were greater than the 'minimal sample size' (i.e. within ±10% of the 'progressive mean'), (ii) values for β were 1.41-1.46 (i.e. close to the value for a sphere of 1.38), and (iii) values for K were 1.02-1.39 (i.e. close to a normal distribution).

### Biochemical fractionation

Large nuclear RNP particles were purified essentially as described by Sperling et al. (1985). Cells ($10^8$/25 ml medium) were grown (15 minutes), regrown (30 or 60 minutes) ± 2.5 mM Br-U and ± [$^3$H]cytidine (250 μCi/ml; 23 Ci/mmol), pelleted, washed in PBS and then PB, swollen (15 minutes; 0°C) in 20 ml hypotonic PB, broken (15 strokes; tight-fitting 'Dounce' homogenizer), lysed (0.2% Triton X-100), and pelleted (5 minutes; 750 ***g***) through 5 ml 25% glycerol in hypotonic PB. Nuclei were resuspended (10 ml hypotonic PB), repelleted through glycerol, resuspended (1 ml hypotonic PB), and broken by sonication (Sanyo Soniprep 150 with microprobe; maximum amplitude; 10 seconds). After addition of 2 mg tRNA (brewer's yeast), debris was removed (1 minutes; 10,000 ***g***), and the supernatant (0.75 ml) spun on a sucrose gradient (15-45% in hypotonic PB; Beckman SW41 rotor; 90 minutes; 40,000 rpm). 24 fractions (0.5 ml) were collected; fraction 1 contained a pellet, and fractions 8-12 the 200 S particles.

## RESULTS

### Br-U is incorporated into nascent RNA, which moves to the cytoplasm

Preliminary experiments showed that Br-U is both incorporated and transported efficiently. HeLa cells were grown for various times in Br-U, sectioned, and any Br-RNA on the surface of sections immunolabelled with gold particles. A few lone particles were scattered over all parts of the cell; as they were also found at zero time, they represent nonspecific, background, labelling. As growth time increases, clusters of gold particles accumulate over the nucleoplasm (Fig. 1A-C). No label was found over coiled bodies during the first hour. Eventually, clusters fuse into a diffuse network (Fig. 1D), and coiled bodies and the periphery of the few mitotic chromosomes in the population also become labelled. Even after long periods of growth in Br-U, few perichromatin granules, or regions within interchromatin granule clusters, become labelled (Fig. 1C,D; see also Puvion and Puvion-Dutilleul, 1996). After ~10 minutes, the first clusters are seen over the cytoplasm, and then numbers increase (e.g. Fig. 1D). This cytoplasmic labelling will be described in detail elsewhere (F. J. Iborra, D. A. Jackson and P. R. Cook, unpublished work). Labelling in nucleoplasmic clusters marked RNA as it is abolished by RNase A treatment (as described by Iborra et al., 1996), but unaffected by DNase I treatment (500 units/ml in PBS + 5 mM $MgCl_2$ for 1 hour at 37°C). Moreover, it is not due to incorporation into DNA as it is seen both in nonreplicating cells synchronized in $G_1$ phase and without acid denaturation (as described by Hozák et al., 1993).

Growth in high concentrations of Br-U for long periods is toxic. Thus, HeLa cells double every ~22 hours but, following exposure for 1, 2, 5 or 24 hours to the highest concentration of

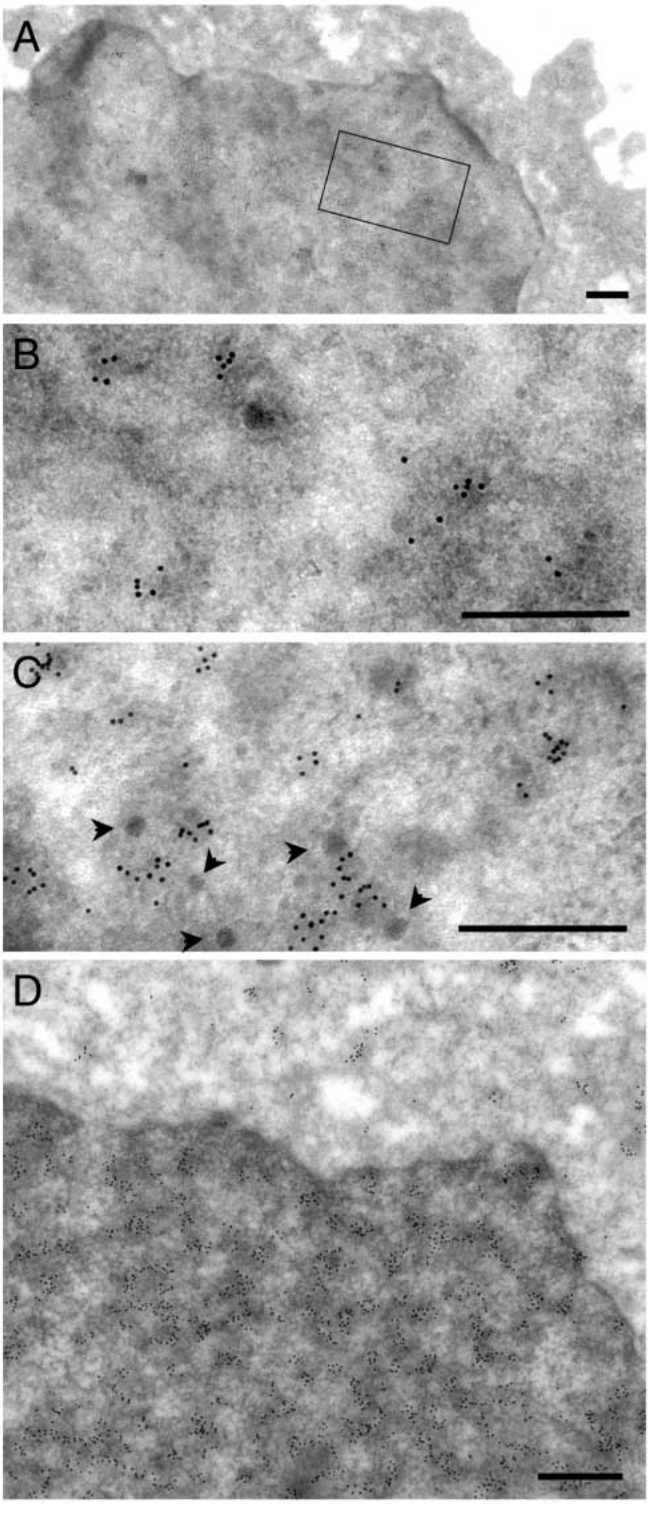


**Fig. 1.** Pathway of Br-RNA from nucleus to cytoplasm. Cells were grown in 2.5 (A,B,C) or 0.5 (D) mM Br-U, fixed, and sites on the surface of sections containing incorporated Br immunolabelled with gold particles (9 nm). Bars: 200 nm. (A) 10 minutes growth in Br-U. (B) Region in rectangle in A. Many particles are found in clusters. (C) 60 minutes growth in Br-U. The number of particles in clusters is higher; perichromatin granules (arrowheads) remain unlabelled. (D) 24 hours growth in Br-U (the concentration used increased doubling time from 23 to 27 hours). Nucleoplasmic clusters are now so numerous they have fused into a diffuse network, but the nuclear membrane is unlabelled. Some clusters are found over the cytoplasm.

Br-U routinely used here (i.e. 2.5 mM), they double after 24.5, 25, 26.4 and 45 hours, respectively. Therefore, cells are usually grown for ≤1 hour in ≤2.5 mM Br-U, when toxic effects are negligible. Moreover, such exposures have little effect on transcription rates; for example, when $G_1$ cells are grown in [$^3$H]adenosine and 2.5 mM Br-U, tritium is incorporated over the first hour into acid-insoluble material at ≥95% the rate of controls grown in 2.5 mM U.

### The quantitative approach

We estimate numbers of nuclear sites as follows. Inspection of images like those in Fig. 1 gives the impression that lone particles reflect an irreducible background labelling, while clusters mark Br-RNA at different stages in the pathway. Therefore we categorized particles as either lone or clustered, where a cluster was defined as >1 particle lying within 40 nm of another (centre-to-centre distance), and normalized numbers relative to area. The number of lone particles over nucleoplasm or cytoplasm (i.e. ~0.9 particles/μm$^2$) did not change with incorporation time or Br-U concentration; however, the total number of particles over various cellular compartments rose (Fig. 2A), due to increased labelling in clusters (Fig. 2B). These results confirm that lone particles reflect a background, while clusters mark Br-RNA.

Gold particles lie on the surface of sections illustrated in Fig. 1, and total numbers in a nucleus can be calculated using standard stereological techniques, assuming random sectioning (Williams, 1977). We also immunolabel before embedding (e.g. Fig. 4) so particles are distributed throughout sections; then, particle densities imaged in two-dimensions are directly related to three-dimensional densities. Both approaches suffer several drawbacks (Griffiths, 1993). First, precise quantitation of antigen concentrations in different sites is impossible, as antigenicity may vary from site to site. Second, an immunolabelling gold particle can lie up to 23 nm away from the antigen it marks, as it might be connected to it through two molecules of immunoglobulin and one of Protein A (lengths of ~9, ~9 and ~5 nm, respectively). In practice, resolution is almost always better than this, so no corrections have been made for such errors. However, a 10% overestimate of the radius of a spherical object will lead to a 10% underestimate of the numbers of that object in the nucleus. Note also that two particles lying within 40 nm of each other, our smallest 'cluster', will usually mark two different epitopes. Third, a nascent nucleoplasmic transcript (average length ~8,400 nucleotides) is probably compacted into several nanometers, even though it could potentially stretch ~3 μm (i.e. a significant fraction of nuclear diameter). Fourth, particle numbers in a cluster reflect the amount of Br-RNA in the target area over a limited range, as sites soon become saturated with particles. Thus, after 10 minutes growth in 2.5 mM Br-U, a cluster with a diameter of ~65 nm typically contains ~5 particles spaced ~20 nm apart, which is the tightest packing attainable (Iborra and Cook, 1998). Therefore, measurements of cluster number are usually more informative than measurements of particle number. Fifth, it proves difficult to combine preservation of ultrastructural detail with efficient immunolabelling (Griffiths, 1993); here, we deliberately maximize immunolabelling efficiency, with some loss of detail.

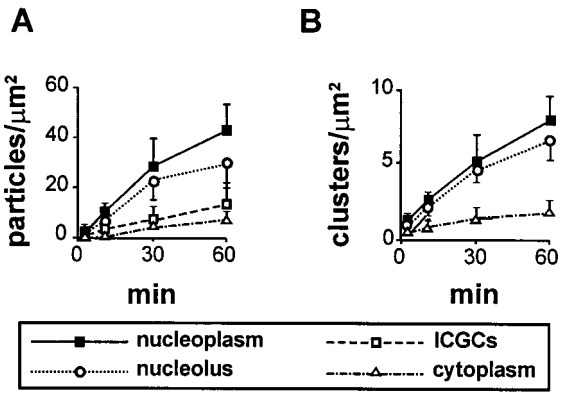


**Fig. 2.** Br-U incorporation increases with time. Cells were grown in 2.5 mM Br-U for different times, fixed, sites on the surface of sections containing Br-RNA immunolabelled with gold particles (9 nm), and the numbers of particles (A) and clusters (B) over different regions counted. ICGCs: interchromatin granule clusters. Error bars: ± s.d.

### Nucleolar incorporation is specially sensitive to Br-U concentration

Permeabilized cells incorporate Br-UTP into RNA at ~80% of the rate of the natural analogue; this shows that the major polymerizing activity (i.e. RNA polymerase II) is relatively unaffected by the analogue. However, nucleoli incorporate Br-U poorly, probably for two reasons. First, 45S rRNA contains only 16% U, which is less than the U-rich extranucleolar transcripts (Lewin, 1974). Second, the following experiment suggests that RNA polymerase I prefers to incorporate UTP rather than Br-UTP. Cells were grown for 30 minutes in a fixed concentration of U+Br-U, but decreasing concentrations of Br-U, before Br-RNA was immunolabelled. The number of particles over the nucleolus and nucleoplasm fell by ~140× and 14×, respectively (Table 1). This is consistent with polymerase I incorporating less Br-UTP as the availability of UTP increases. Nucleoli also incorporate [$^3$H]C more efficiently than Br-U (see Tables 6 and 7). (Note that polymerase I will use Br-UTP in the absence of UTP; for example, when only Br-UTP is supplied to permeabilized cells, nucleoli become labelled more intensely than the nucleoplasm.) This poor nucleolar incorporation is to our advantage, as the 'background' ribosomal transcripts are not as well labelled as the nucleoplasmic transcripts that concern us here.

### Distinguishing extra-nucleolar transcription sites from downstream sites

After growth in Br-U for more than a few minutes, most nucleoplasmic clusters will mark transcripts moving away

**Table 1. Br-U is incorporated into nucleoli poorly**

| | Particles/μm$^2$ | |
|---|---|---|
| Growth conditions | Nucleolus | Nucleoplasm |
| 2.5 mM Br-U | 20±12 | 28±13 |
| 1.25 mM Br-U + 1.25 mM U | 0.7±0.8 | 3.4±0.9 |
| 0.5 mM Br-U + 2.0 mM U | 0.14±0.3 | 1.9±0.7 |

Cells were grown for 30 minutes in Br-U±U (combined molarity 2.5 mM), fixed, Br-RNA on the surface of sections immunolabelled with gold particles (9 nm), and the numbers of particles/μm$^2$ over nucleolus and nucleoplasm counted.

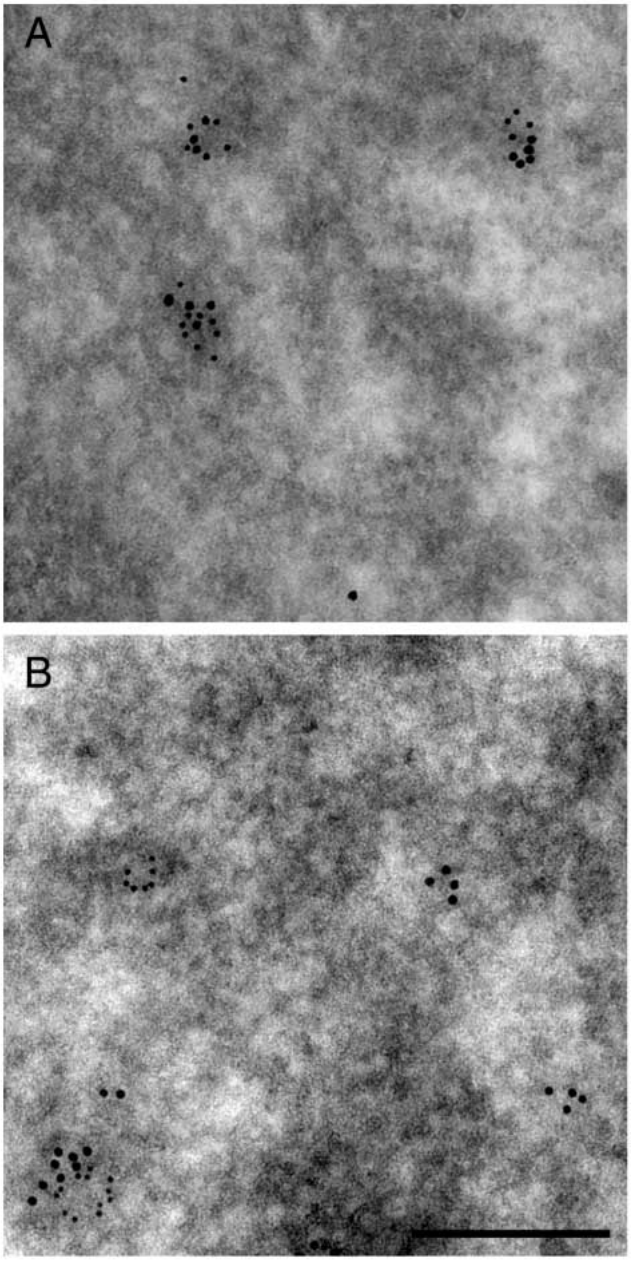


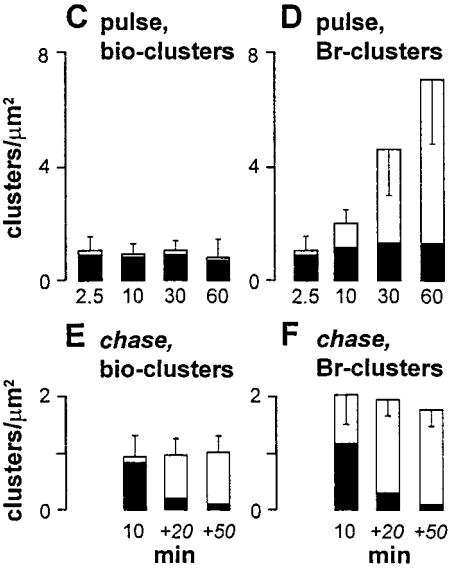


**Fig. 3.** Distinguishing synthetic from downstream sites. Cells were grown (the pulse) in 5 mM Br-U for 2.5 minutes, or in 2.5 mM Br-U for 10, 30 or 60 minutes; in some cases, cells were washed after 10 minutes and regrown for *20* or *50* minutes without Br-U (the *chase*). Next, cells were permeabilized, allowed to extend nascent transcripts in bio-CTP, before sites containing Br- and bio-RNA were marked with 9 and 5 nm gold particles, respectively. A nucleoplasmic Br-cluster was considered to contain bio-RNA (and vice versa) if a gold particle in one cluster lay within 40 nm of a gold particle in the other cluster; fractions containing both kinds of cluster are indicated by shaded areas in C-F. C-F include some data from Jackson et al. (1998). (A) Growth in Br-U for 2.5 minutes, lysis, and extension in bio-CTP. The 3 clusters contain both large and small particles (marking Br-RNA and bio-RNA, respectively). (B) Growth in Br-U for 10 minutes, followed by a *chase* of *50* minutes, lysis, and extension in bio-CTP. Some clusters contain only large particles, others only small particles, and still others contain both. Bar: 200 nm. (C) The number of bio-clusters (marking transcription sites) remains constant, irrespective of the length of the Br-U pulse. At all times, ~85% bio-clusters also contain Br-RNA (shaded fraction). (D) The number of downstream sites (i.e. containing only Br-RNA; unshaded fraction) increases with time, as the number of transcription sites (i.e. containing both bio- and Br-RNA; shaded fraction) remains constant. (E) After a 10 minutes pulse in Br-U and *chases* of *20* and *50* minutes, transcription sites (i.e. bio-clusters) exponentially lose Br-RNA (shaded fraction). Note scale is doubled. (F) After a 10 minutes pulse in Br-U and *chases* of *20* and *50* minutes, downstream sites (i.e. Br-clusters without bio-RNA; unshaded) continue to appear exponentially. Note scale is doubled.

from synthetic sites. We distinguished these downstream sites from transcription sites by double-labelling. Cells were grown in Br-U for 2.5-60 minutes, permeabilized, and allowed to extend nascent Br-RNA chains in bio-CTP; then, sites containing Br-RNA and bio-RNA were labelled with 9 and 5 nm gold particles, respectively. Under these in vitro conditions, engaged polymerases extend existing transcripts by ~250 nucleotides, no new transcripts are initiated, and the resulting bio-RNA remains in synthetic sites (Iborra et al., 1996). Therefore, clusters of small particles (‘bio-clusters’) mark synthetic sites, while clusters of large particles (‘Br-clusters’) mark both synthetic and downstream sites. As expected, most sites initially contain both bio-RNA and Br-RNA (Fig. 3A); most transcription sites active after lysis were active in vivo a moment earlier. A cluster was considered to contain both Br-RNA and bio-RNA if a particle in a ‘Br-cluster’ lay within 40 nm of a particle in a ‘bio-cluster’. Additional downstream sites containing only Br-RNA appear later (see below).

We first analyzed how closely bio- and Br-RNA were initially associated in transcription sites after a Br-U pulse of 2.5 minutes. Complete overlap between the two kinds of cluster would be observed if the underlying structures containing the analogues had identical diameters and coincident centres of gravity. However, the two types of cluster did not colocalize exactly; their centres of gravity lay, on average, 29 nm apart (not shown). This probably reflects incorporation of the two analogues into different parts of one transcript (or group of transcripts). Only ~85% ‘bio-clusters’ initially contained Br-RNA (Fig. 3C, 2.5

minutes, shaded fraction), and vice versa (Fig. 3D, 2.5 minutes, shaded fraction). It can be calculated that if the centre of every 'Br-cluster' (diameter 80 nm) lay 29 nm away from the centre of a 'bio-cluster' (diameter 80 nm), random sectioning would give 82% overlap, close to the value seen.

We next counted the number of transcription sites; at all times, there was ~1 'bio-cluster'/$\mu m^2$ (Fig. 3C). Assuming random sectioning and underlying sites have the same diameter as the clusters that mark them (i.e. 80 nm), we can use standard stereological procedures to calculate that there are 5,000 sites in the three-dimensions of a nucleus (see Table 4).

How quickly do downstream sites appear? As cells are grown in Br-U for longer, the density of 'Br-clusters' increases (Fig. 3D). This increase is entirely due to the appearance of 'Br-clusters' that lack bio-RNA (i.e. in Fig. 3D, the unshaded fraction increases from 2.5 to 60 minutes). ~0.12 such downstream clusters/$\mu m^2$ appear every minute, equivalent to only ~600/minute in a nucleus.

We next determined how quickly Br-RNA left transcription sites for downstream sites using a pulse-chase experiment (Fig. 3E). After a 10 minute pulse, ~85% 'bio-clusters' contain Br-RNA, but then Br-RNA is lost (in Fig. 3E, the shaded fraction falls). Simultaneously, downstream sites appear (in Fig. 3F, the unshaded fraction increases). After a chase of 50 minutes, little Br-RNA remains at primary transcription sites (Fig. 3F, shaded fraction). Quantitative analysis shows that Br-RNA disappears with first-order kinetics (i.e. roughly at a rate of $-0.06$ $minute^{-1}$), before appearing in downstream sites at much the same rate (i.e. $+0.05$ $minute^{-1}$).

## Br-RNA is initially contained in a few downstream sites in the nucleoplasm

Our methods are sufficiently sensitive to detect most transcription sites, as the same numbers are seen: (i) after growth for 1.25 or 2.5 minutes in 2.5, 5 or 10 mM Br-U; and (ii) using a different precursor, biotin-CTP, and detection system (Iborra et al., 1996; Jackson et al., 1998). But are all downstream sites detected? If many were going undetected, increasing the bromine content in individual transcripts should raise more above the threshold of detection. However, the same density of clusters is seen, irrespective of Br-U content (Table 2).

**Table 2. Most downstream sites are detected**

| Br-U concentration (mM) | Clusters/$\mu m^2$ ('high') | Particles/$\mu m^2$ ('low') |
|---|---|---|
| 2.5 | 8.2±4 | 9±2 |
| 5 | 7.8±2 | 26±6 |
| 10 | 7.9±1 | 35±5 |

Cells were grown in different concentrations of Br-U for 1 hour so that most Br-RNA had left transcription sites for downstream sites; after fixation, Br-RNA on the surface of sections was immunolabelled with gold particles (9 nm), and numbers of particles and clusters counted. A 'high' concentration of primary antibody was used to measure cluster density (to optimize cluster detection); then, sites become so tightly packed with gold particles that the number of particles/$\mu m^2$ cannot increase with increasing Br-U concentration. A 'low' (i.e. one-tenth) concentration of primary antibody was used to measure particle densities, so that variations in Br-U content could be seen. Cluster density (reflecting the number of downstream sites) remains constant despite the increase in particle density (reflecting Br-U content).

**Table 3. Diameters of sites containing Br-RNA and SR antigens**

| Site (labelling conditions) | Cluster size ± s.d. (nm) | | Diameter corresponding sphere (nm) |
|---|---|---|---|
| | Major axis | Minor axis | |
| Br-RNA in nucleoplasm | | | |
| 2.5 minutes, 2.5 mM Br-U | 63±22 | 39±19 | 77 |
| 10 minutes, 2.5 mM Br-U | 60±20 | 38±13 | 75 |
| 30 minutes, 2.5 mM Br-U | 65±27 | 41±16 | 79 |
| 30 minutes, 1.25 mM Br-U + 1.25 mM U | 59±16 | 40±11 | 77 |
| 30 minutes, 0.5 mM Br-U + 2.0 mM U | 60±11 | 39±8 | 76 |
| 60 minutes, 2.5 mM Br-U | 65±20 | 40±14 | 79 |
| SR clusters in nucleoplasm | 66±15 | 42±10 | 83 |
| Br-RNA at membrane | | | |
| 10 minutes, 2.5 mM Br-U | 55±16 | 33±7 | 67 |
| 60 minutes, 2.5 mM Br-U | 76±27 | 51±18 | 94 |

Cells were grown for various times in Br-U±U, fixed, and Br-RNA on the surface of sections immunolabelled with gold particles (9 nm). Lengths of major and minor axes of >60 clusters of particles were measured, and diameters of equivalent spheres calculated.

If most downstream sites containing Br-RNA are detected, it follows that they are produced in each nucleus at a surprisingly low rate (i.e. ~600/minute; see above). Therefore, it is unlikely that each contains only one message, as such a production rate cannot sustain cytoplasmic mRNA levels (see Discussion).

## Nucleoplasmic sites containing Br-RNA have apparent diameters of ~80 nm

Transcription and downstream sites are both remarkably uniform in size; irrespective of labelling time, major and minor axes of clusters remain constant (Table 3). Br-RNA does not accumulate in sites that grow ever larger (like clusters at the membrane; Table 3); rather, it is made in sites with diameters of ~80 nm, before it moves downstream in, or to, sites of similar size. As we feared that Br-RNA containing considerable amounts of bromine might be treated aberrantly, we also measured diameters after growing cells in progressively less Br-U. However, diameters remained unchanged even after growth in 0.5 mM Br-U plus 2 mM U (Table 3), a concentration that does not affect growth.

## RNA in downstream nucleoplasmic sites can be extracted with 2 M NaCl

Completed transcripts, but not nascent ones, can be extracted from nuclei by 2 M NaCl (Jackson and Cook, 1985; Verheijen et al., 1988). Therefore, we tested the sensitivity of Br-RNA to extraction; cells were grown in 2.5 mM Br-U for 1 hour to label many downstream sites, and extracted; then, as residual material is poorly imaged by the techniques used for Fig. 1 (Penman, 1995), we immunolabelled before embedding so that gold particles are spread throughout the three dimensions of sections (Fig. 4). Clusters of particles are now associated with residual material, and their diameter (i.e. 71 nm) is similar to that found by postembedment labelling (i.e. 75-79 nm; Table 3). Although extraction exposes more Br-RNA and increases the number of particles in a cluster, stereological analysis shows that it reduces the number of clusters in a nucleus from

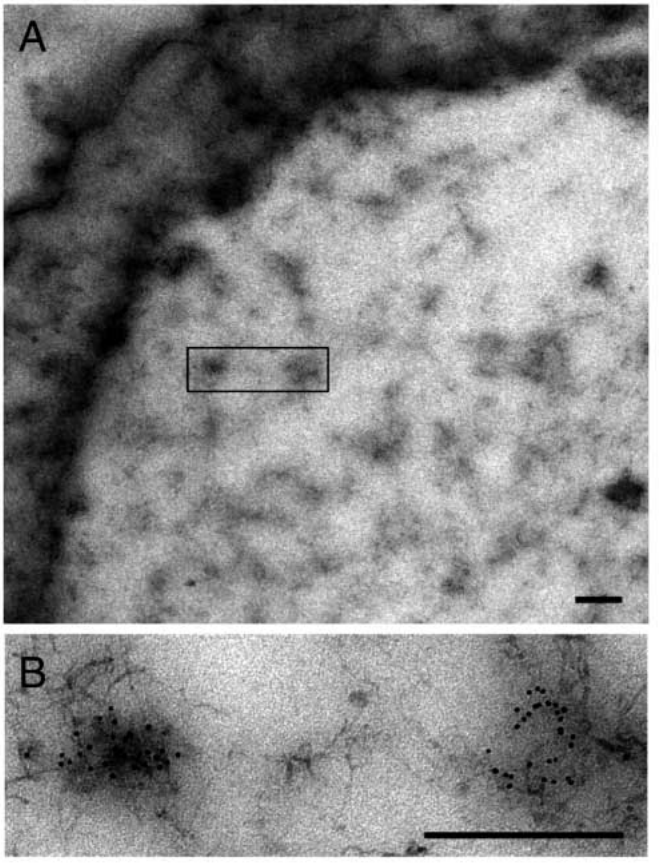


**Fig. 4.** Some sites containing Br-RNA resist extraction with 2 M NaCl. Bars: 200 nm. (A) Encapsulated cells were grown in 2.5 mM Br-U for 1 hour, lysed in 2 M NaCl, fixed, Br-RNA immunolabelled with 5 nm particles before embedding, and 200 nm sections prepared. A fibrogranular network extends throughout the nucleoplasm. (B) Region in rectangle in A; clusters mark Br-RNA that resists extraction.

36,000 to 2,900, close to the number (i.e. 5,500) of transcription sites (Table 4). This is consistent with downstream sites being sensitive to extraction, and so structurally distinct from transcription sites.

## Both transcription and downstream nucleoplasmic sites contain a subset of SR proteins

SR proteins are a group of splicing factors found in nuclear 'speckles' and transcription sites; they are also associated with transcripts as they move to pores (e.g. Roth et al., 1990; Alzhanova-Ericsson et al., 1996; Colwill et al., 1996; Neugebauer and Roth, 1997; Cáceres et al., 1997; reviewed by Kramer, 1996). Different antibodies are available that detect different subsets of this group of proteins and one, monoclonal antibody 104, recognizes a phosphorylated subset (Roth et al., 1990). We found that this subset is concentrated in ~90,000 nuclear 'SR-clusters' or 'SR sites' with diameters of 83 nm (Fig. 5A; Tables 3, 4). Some of these clusters touch the nuclear membrane (i.e. 0.17±0.2/μm membrane). This antibody does not detect SR proteins in interchromatin granule clusters, unlike others. Double-labelling shows that it labels both transcription and downstream sites (Fig. 5B,C).

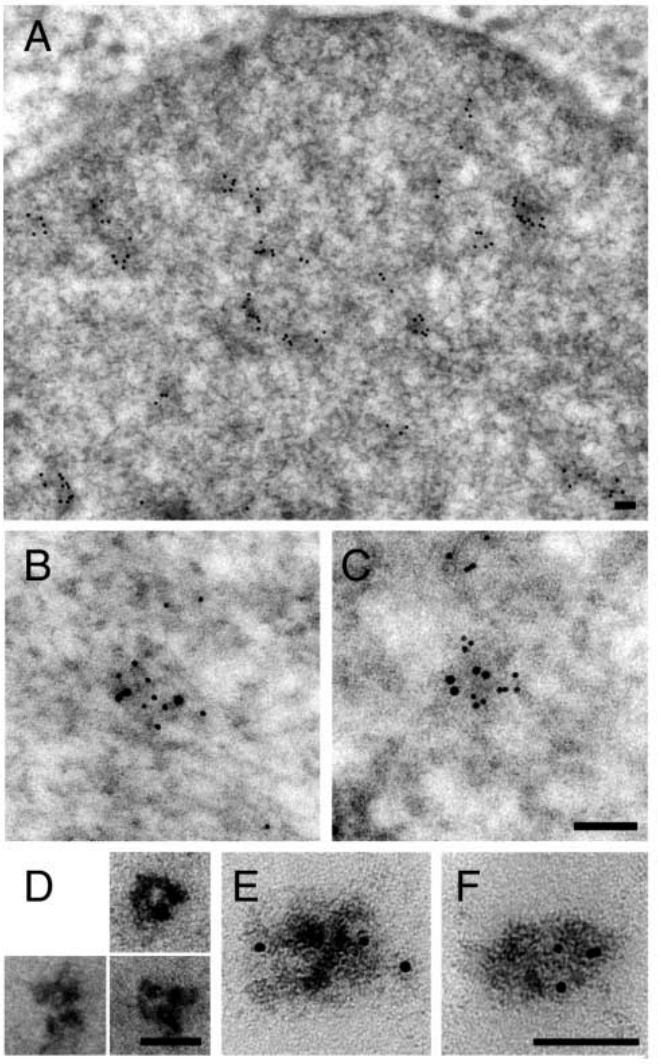


**Fig. 5.** Br-RNA is associated with a subset of SR antigens (marked by 9 nm particles) in large nuclear ribonucleoprotein particles. Bars: 50 nm (B,C and E,F at same magnification). (A) SR antigens are clustered within nuclei. Particle clusters have the range of diameters expected if spheres of ~83 nm are sectioned at random. (B) SR antigens colocalize with transcription sites containing bio-RNA (marked by 5 nm particles). The central cluster contains both 5 and 9 nm particles. (C) SR antigens are found in downstream sites containing Br-RNA (marked by 5 nm particles). Cells were grown in 2.5 mM Br-U for 1 hour before immunolabelling, to give time for most Br-RNA to leave primary transcription sites. The central cluster contains both Br-RNA and SR antigens, while the upper contains only Br-RNA. (D) A gallery showing 3 large nuclear ribonucleoprotein particles. Cells were disrupted, spun in a sucrose gradient, fractions 8-12 pooled, and material stained and imaged. Particles have structures typical of large nuclear ribonucleoprotein particles. (E,F) Cells were grown in 2.5 mM Br-U for 30 minutes, material in fractions 8-12 collected as in D, and SR antigens (E) or Br-RNA (F) immunolabelled.

## Br-RNA is packaged into 200 S particles

Transcripts at different stages of the pathway are packaged into various ribonucleoprotein particles that can be isolated on sucrose gradients, including small particles, functional

**Table 4. Cluster density (measured per unit area, or per unit length along the nuclear membrane), and calculated numbers of sites per nucleus (see Materials and Methods)**

| Labelling conditions | Site labelled | Clusters/μm$^2$ | Clusters/μm | Sites/nucleus |
|---|---|---|---|---|
| Bio-CTP in vitro | Transcription | 1.0±0.3 | | 5,000 |
| 2.5 minutes Br-U in vivo | Transcription | 1.1±0.5 | | 5,500 |
| 60 minutes Br-U in vivo | Transcription + downstream nuclear pores | 7.1±2.2 | 0.8±0.6 | 36,000 |
| 60 minutes Br-U in vivo, extracted | Transcription, nuclear pores | 1.3±0.6* | 3.7±0.2* | 2,900<br>4,800 |
| Anti-SR antibody | SR (splicing) proteins | 18.0±7 | | 90,000 |

*Measured in 2-D images of 3-D sections, so values of clusters/μm and clusters/μm$^2$ given correspond to values in 2- and 3-dimensions, respectively.

spliceosomes, and large tetrameric particles of 200 S (Dreyfuss et al., 1993; Sharp, 1994). A low-resolution structure is available for the 200 S particles, which have a diameter of ~50 nm; they contain small nuclear RNPs and several splicing factors, including SR proteins (Yitzhaki et al., 1996; Sperling et al., 1997). Their size and SR content suggested that the 200 S particles might be derived from downstream sites, so we investigated whether they contained Br-RNA. Cells were grown in Br-U for 30 minutes, nuclei isolated, and their contents spun on a sucrose gradient. 200 S particles are found in the expected part of the gradient (Fig. 5D), and immunolabelling shows that 95% contain SR antigens (Fig. 5E), and 23% contain Br- RNA (Fig. 5F; Table 5). This is simply explained if 200 S particles are derived from SR sites, a fraction of which contain Br-RNA.

## Downstream sites, SR sites, and 200 S particles are directly related

These results suggest that downstream sites containing Br-RNA are a subset of ~90,000 SR sites, and that 200 S particles are derived from SR sites. Therefore, we investigated whether Br-RNA flowed through the three kinds of structure with similar kinetics. Cells were grown for 30 or 60 minutes in Br-U, and the percentages of 'SR clusters' or 200 S particles containing Br-RNA counted; observed values were close to the numbers expected if ~90,000 downstream sites became labelled at a steady rate of ~600/minute (Table 5).

## Br-RNA can accumulate aberrantly at nuclear pores

Little Br-RNA is found at the nuclear periphery after growth in 0.5 mM Br-U for 24 hours (Fig. 1D). However, Br-RNA containing more bromine accumulates abnormally just inside pores. Thus, after growth in 2.5 mM Br-U for only 1 hour, clusters of particles are seen over the internal face of the nuclear membrane, apparently awaiting export through pores (Fig. 6A). These clusters colocalize with nucleoporin p62 (Fig. 6B), a component of pores (e.g. Buss and Stewart, 1995). They also resist extraction with 2 M NaCl, and often seem to form a queue along fibrils that stretch into the interior (Fig. 6C). These fibrils are probably remnants of the basket attached to the internal face of the pore (Davis, 1995; Panté and Aebi, 1996; Nigg, 1997). Quantitative analysis shows that the number of clusters along each micron of membrane rises to a maximum after 30 minutes (Fig. 7A), when there are 3.7 clusters/μm$^2$ of membrane, equivalent to 4,800 clusters per nucleus (Table 4). This is similar to the density of pores in a mammalian cell (Bastos et al., 1995), suggesting that some highly substituted Br-RNA is associated with every pore.

This saturation eventually causes highly substituted RNA to accumulate within ~400 nm of the membrane. This is clearly seen when Br-RNA is chased away from the interior to the periphery (Fig. 6D). Most Br-RNA in this peripheral rim can be extracted with 2 M NaCl, unlike the Br-RNA associated with fibrils attached to pores.

**Table 5. Relationship between 'SR sites', 200 S particles and downstream (nucleoplasmic) sites**

| | % Sites or particles containing Br-RNA | | |
|---|---|---|---|
| Labelling period (minutes) | SR sites (observed) | 200 S particles (observed) | Downstream sites (calculated) |
| 30 | 21 | 23 | 19 |
| 60 | 47 | 38 | 37 |

Cells were grown in 2.5 mM Br-U for 30 or 60 minutes, images like those illustrated in Fig. 5C,F collected, and the percentage of 'SR clusters' or 200 S particles containing Br-RNA counted. The percentage of downstream sites that contained Br-RNA was also calculated, assuming 600 new sites containing Br-RNA are added each minute to 90,000 downstream sites, as 600 unlabelled sites/minute are removed by export to the cytoplasm.

## Br-RNA can dock normally at pores

Both this saturation and back-up are not seen when Br-RNA contains less bromine. For example, when cells are exposed to 2.45 mM Br-U plus 0.05 mM U for 30 minutes, a concentration that has no effect on growth, there are 0.16 clusters/μm membrane, equivalent to saturation of ~18% pores (calculated as above). These clusters have similar diameters to downstream sites in the interior, but they resist extraction with 2 M NaCl (Fig. 6E). However, Br-RNA remains associated with the SR proteins detected by antibody 104; similarly sized SR clusters are found at pores (Fig. 6F) in similar numbers. Intriguingly, Br- and SR-clusters are concentrated ~200 nm away from the membrane (Fig. 7B; not shown), suggesting that downstream sites dock on to the basket (see also Daneholt, 1997; Panté et al., 1997). As so few particles are seen directly over pores (Fig. 7B), Br-RNA must be transported rapidly through the membrane (Daneholt, 1997; Panté et al., 1997).

## Export to the cytoplasm

We next used autoradiography to investigate how Br-U affected transport. Cells were grown for 1 hour in [$^3$H]C so that the label was incorporated into newly made RNA, and autoradiographic grains over different compartments were counted. 81% grains were over nuclei, 24% over nucleoli (Table 6; see also Harris

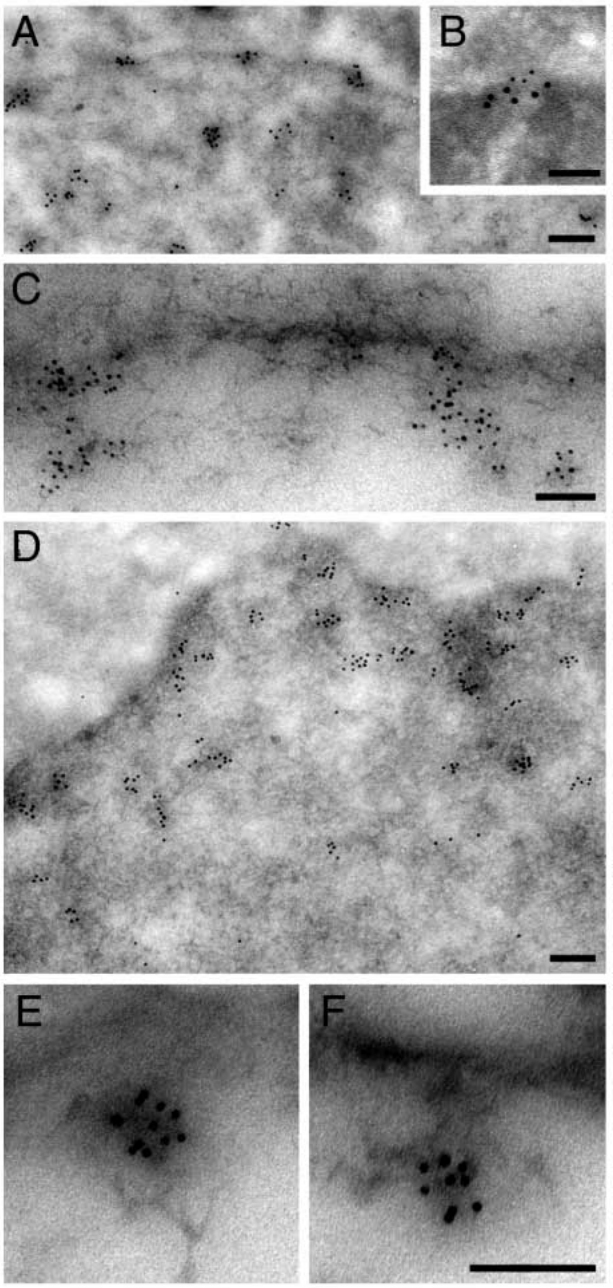


**Fig. 6.** Br-RNA at nuclear pores. Bars: 200 nm (A-D) and 100 nm (E,F). (A) Cells were grown in 2.5 mM Br-U for 1 hour, fixed, and Br-RNA on the surface of sections immunolabelled with 9 nm particles. This section is chosen to illustrate the 4 clusters along the internal face of the nuclear membrane; the one on the right straddles the pore. (B) As in A but nucleoporin p62 also labelled with 5 nm particles. (C) Cells were grown as in A, extracted with 2 M NaCl, and Br-RNA immunolabelled with 5 nm particles before embedding and sectioning (200 nm). Groups of clusters seem to mark Br-RNA that is backing up at the pores. (D) Cells were grown in 2.5 mM Br-U for 1 hour, washed, regrown in 0.5 mM uridine for 15 minutes, rewashed, and regrown for 22.75 hours. Few clusters are now seen over the nuclear interior, but many are concentrated at the nuclear periphery; some are found over the cytoplasm. (E) Cells were grown in 0.5 mM Br-U plus 0.05 mM U for 1 hour, and extracted and immunolabelled as in C. A discrete cluster of particles lies close to the membrane; series of clusters that appear to back up at the pore (as in C) are never seen. (F) As E, except particles mark SR proteins.

**Table 6. The effects of Br-U on incorporation of [$^3$H]C into RNA, and transfer of [$^3$H]RNA to the cytoplasm**

| | 1 hour pulse | 1 hour pulse (+ aphi) | 1 hour pulse (+ aphi + Br-U) | 1 hour pulse (+ aphi + Br-U), 23 hour chase |
|---|---|---|---|---|
| Nucleus | 81 | 83 | 65 | 26 |
| Nucleolus | 24 | 25 | 21 | 2 |
| Nucleoplasm | 57 | 58 | 44 | 24 |
| Cytoplasm | 19 | 20 | 16 | 50 |
| Total | 100 | 103 | 81 | 76 |

Cells were grown for 1 hour in [$^3$H]C ± aphidicolin (aphi; used to inhibit incorporation into DNA) ± 2.5 mM Br-U (the pulse), and some were washed and regrown for 23 hours in the absence of any additives other than 0.5 mM U (the chase). After fixation and acid extraction, autoradiographs were prepared, and the numbers of silver grains (marking [$^3$H]RNA) over different compartments were counted. Results are expressed as a percentage of grain counts found over cells grown for 1 hour in [$^3$H]C.

**Table 7. Relative amounts of Br-RNA in different compartments after a 1 hour pulse with 2.5 mM Br-U, and a 23 hour chase**

| | Volume | | Labelling: 1 hour pulse | | Labelling: 1 hour pulse, 23 hour chase | |
|---|---|---|---|---|---|---|
| | $\mu m^3$ | % | Particles/$\mu m^2$ | % | Particles/$\mu m^2$ | % |
| Nucleus | 414 | 38 | 45 | 76 | 32 | 54 |
| Nucleolus | 14 | 1.3 | 34±12 | 7 | 3.9±3 | 1 |
| Nucleoplasm | 400 | 36.7 | 41±17 | 69 | 33±8 | 53 |
| Interior | 349 | 32 | 40±18 | 61 | 9±6 | 11 |
| Rim | 51 | 4.7 | 59±18 | 8 | 284±48 | 42 |
| Cytoplasm | 673 | 62 | 8.5±3.5 | 24 | 2.6±0.6 | 7 |
| Total | 1,087 | 100 | | 100 | | 61 |

Cells were grown, embedded, Br-RNA immunolabelled, particle numbers and areas of each compartment measured, and volumes calculated. The nucleus was divided into nucleolus, a peripheral rim lying within 200 nm of the nuclear membrane, and the nuclear interior (i.e. remaining nucleoplasm). As compartment volumes differ, particle densities were normalized by multiplication with the corresponding volume, before they were expressed as a percentage.

and Watts, 1962). As some [$^3$H]C could be incorporated into DNA, we added also sufficient aphidicolin to inhibit DNA synthesis; this had essentially no effect on grain counts (Table 6). Addition of 2.5 mM Br-U reduced counts over all compartments by ~20% (Table 6). When the pulse was followed by a 23 hour chase, counts over nucleoplasm and nucleolus declined, while those over the cytoplasm rose. This shows that even the high concentration of Br-U used here has only a small effect on the general metabolism of RNA.

We also monitored Br-RNA levels in the different compartments more directly by immunolabelling. After the 1 hour pulse, 76% immunolabelling particles were over nuclei; however, only 7% were over nucleoli, showing that polymerase I prefers to incorporate [$^3$H]C rather than Br-U (compare Tables 6 and 7). During the chase, Br-RNA was lost from both nucleoli and the nuclear interior (falling from 7 to 1%, and 61 to 11%, respectively; see also Fig. 6D), and it seems to turn over normally in the cytoplasm (falling from 24 to 7%). However, it accumulates in the peripheral rim (rising from 8 to 42%), in a space that occupies only ~5% cellular volume. As

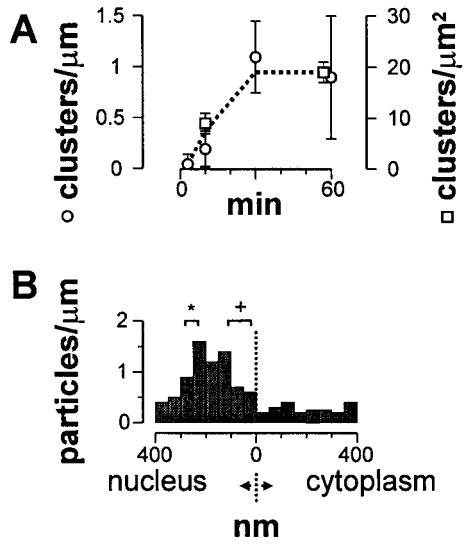


**Fig. 7.** Quantitative analysis of Br-RNA at pores. (A) Pores become saturated with Br-RNA. The numbers of clusters per μm or per $\mu m^2$ of nuclear membrane were measured in images like those in Fig. 6A and C, respectively. Clusters were counted if ≥1 particle in the cluster lay over the membrane. (B) Br-RNA accumulates just inside pores. Cells were grown in 2.45 mM Br-U plus 0.05 mM U for 30 minutes, and images like those in Fig. 6A prepared. All gold particles lying within 400 nm of the membrane were counted, and numbers (per μm along membrane) expressed relative to distance from the membrane. Particles are concentrated ~200 nm away from the membrane. Values indicated were significantly different (Student's *t*-test) at 93 (*) and 95% (+) confidence levels.

a result, 54% Br-RNA remains in the nucleus after the chase, mostly in this rim. We conclude that Br-RNA behaves normally in many respects, except that Br-U is incorporated poorly into nucleoli and that highly substituted Br-RNA accumulates aberrantly at the nuclear periphery.

### Effects of inhibitors on synthesis and transport

The use of inhibitors shows that polymerase II is responsible for most Br-U incorporation. Thus, α-amanitin, an inhibitor of polymerase II, reduced nucleoplasmic labelling from 10±4 to 3.2±0.6 clusters/$\mu m^2$ whereas actinomycin D, a polymerase I inhibitor, had little effect (reducing labelling from 40±14 to 36±18 clusters/$\mu m^2$; not shown). These results obtained after labelling with Br-U are similar to those obtained after labelling with [$^3$H]uridine (Hesketh and Pryme, 1991), so in these respects Br-RNA behaves much like [$^3$H]RNA.

## DISCUSSION

### A method for labelling the pathway that transcripts take to the cytoplasm

Various methods have been used to map the pathway that transcripts take from nucleus to cytoplasm; each has advantages and disadvantages. For example, after growth in tritiated precursors, incorporated analogues can be tracked by autoradiography; this has the great advantage that marked transcripts behave like natural ones. Natural transcripts can also be tracked using in situ hybridization (e.g. Lawrence et al., 1989; Huang and Spector, 1991; Zachar et al., 1993), but, like autoradiography, with poor resolution. Microinjecting RNA attached to gold particles allows direct visualization by electron microscopy (e.g. Dworetzky and Feldherr, 1988; Panté et al., 1997), but attached transcripts are inevitably introduced at unknown points in the pathway. We now describe a new method; HeLa cells are grown in Br-U so that the analogue is incorporated into RNA and exported to the cytoplasm, before Br-RNA is localized by immunogold labelling. The method provides high resolution and sensitivity, probably because individual transcripts contain many tens of epitopes (i.e. bromines), and not the one commonly found in protein antigens. It has the disadvantage, as does microinjection of RNA-gold particles, that the cell has to deal with unnatural transcripts. This inevitably begs the question, to what extent does Br-RNA behave differently from RNA?

Growth in high concentrations of Br-U for long periods is toxic. Toxicity could result from reduced transcription. Three pieces of evidence suggest that extra-nucleolar polymerases, the ones with which we are mainly concerned, incorporate the analogue almost normally. (i) After growth in 2.5 mM Br-U and [$^3$H]cytidine, the two labels become intermingled in the same transcripts, since they copurify when Br-RNA is selected using anti-Br antibodies (Jackson et al., 1998). (ii) The presence of 2.5 mM Br-U reduced the initial rate of incorporation of [$^3$H]adenosine and [$^3$H]cytidine into RNA by ≤20% (see Results, and Tables 6 and 7). (iii) Polymerases in permeabilized cells elongate at ~80% of the normal rate when Br-UTP completely replaces UTP (Iborra et al., 1996). Therefore, it seems likely that toxicity results from abnormal metabolism later in the pathway, for example during splicing and/or translation (Sierakowska et al., 1989; Wansink et al., 1994; Schmittgen et al., 1994). Even so, we have established a set of conditions that allows efficient detection of Br-RNA with little effect on growth. Growth in 2.5 mM Br-U for 2.5-60 minutes enables Br-RNA at the first steps to be detected; short exposures have no detectable effect, while the longest marginally increases doubling time from 22 to 24.5 hours. We also routinely use lower Br-U concentrations that do not affect growth. Except for some accumulation at the nuclear periphery, nucleoplasmic Br-RNA behaves much like natural RNA.

Using this method, we find that Br-RNA passes through three distinct nuclear compartments (i.e. transcription, downstream and docking sites) on its way to the cytoplasm (Fig. 8). Primary transcription sites are the sole ones to contain labelled transcripts after growth in Br-U for ≤2.5 minutes (Fig. 3; Jackson et al., 1998). Then, progressively more Br-RNA enters downstream sites (Fig. 3D), before reaching docking sites just inside pores and exiting to the cytoplasm (Fig. 1D). Little Br-RNA is seen in transit through pores, presumably because it occurs so quickly. Even after 24 hours growth in 0.5 mM Br-U, only ~20% docking sites are occupied with Br-RNA (Fig. 1D). However, after growth in 2.5 mM Br-U, all pores soon become occupied with Br-RNA (Figs 6A, 7A) and Br-RNA backs up (aberrantly) at a fourth site, just inside the nuclear membrane (Fig. 6D, Table 7). After long periods in both high and low concentrations, Br-RNA also appears in additional nucleoplasmic sites (e.g. coiled bodies, parts of interchromatin granule clusters, and perichromatin granules). Each compartment has its own characteristic dimensions and sensitivity to extraction with 2 M NaCl. We find that a subset

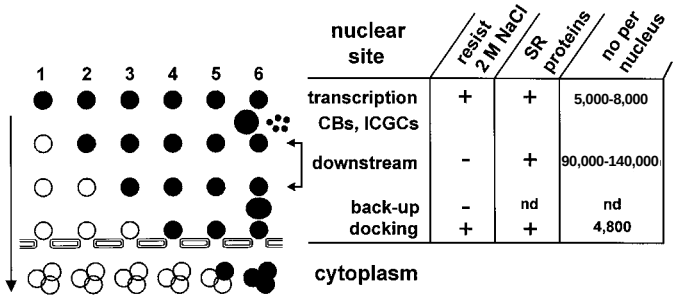


**Fig. 8.** A model for the path of Br-RNA to the cytoplasm. There is a constant flux (arrow) of transcripts from transcription sites (top circles), through downstream sites and pores to the cytoplasm. After a brief pulse (e.g. Br-U for <2.5 minutes in vivo, or extension in bio-CTP in vitro) label (filled circle) is incorporated only into transcription sites (1). After growth for longer in Br-U, progressively more downstream sites become labelled (filled circles), until some Br-RNA reaches the pore and the cytoplasm (2-5). Eventually, Br-RNA forms a diffuse network in the nucleus, accumulating in many regions that are not initially labelled (e.g. coiled bodies, CBs; interchromatin granule clusters, ICGCs); when present in high concentrations, Br-RNA also backs up at the pore (6). Some properties of the different nuclear sites are illustrated on the right (numbers of transcription and downstream sites are calculated using diameters of 80 or 50 nm). nd: not done.

of SR antigens detected by one particular monoclonal antibody are excellent markers of this pathway. Various different SR proteins have been found previously at the appropriate sites (e.g. Roth et al., 1990; Romac and Keene, 1995; Alzhanova-Ericsson et al., 1996; Colwill et al., 1996; Neugebauer and Roth, 1997; Cáceres et al., 1997).

## Downstream sites

Br-RNA is found in surprisingly few downstream sites. Do we fail to detect many such sites because they lie below the threshold of detection? This seems unlikely because increasing the Br-U concentration from 2.5 to 10 mM should raise more sites above the threshold, but no more are seen (Table 2). Our methods could be sufficiently sensitive if each site contains many transcripts (see below), and if each Br-RNA molecule in a site contains many brominated residues (as it probably does). These sites have discrete diameters of ~80 nm, which also remain constant over a range of Br-U concentrations (Table 3).

During growth in 2.5 mM Br-U, downstream sites initially appear at a steady rate of 0.12 sites/minute per $\mu m^2$ of section (Fig. 3D), equivalent to 600 new sites/minute in a nucleus. How many transcripts does each contain? When considering the possibilities, we assume that (i) ~75,000 transcripts are made at any one time in extra-nucleolar regions of a HeLa nucleus (mainly by polymerase II), (ii) a typical primary transcript of ~8,400 nucleotides is completed in ~7 minutes, (iii) one-twentieth the mass of the primary message reaches the cytoplasm as message (three out of four primary transcripts are completely degraded, and splicing removes four-fifths the length of the remainder), (iv) there are ~$10^6$ messages in the cytoplasm (with lengths of 1,500 nucleotides and half lives of 500 minutes), and (v) cells divide every 22 hours. These values lie within accepted ranges (e.g. Cox, 1976; reviewed by Jackson et al., 1998). Then, it can be calculated that ~$10^6$ messages/cell can only be maintained if ~8,000 primary transcripts are made in the nucleus and ~2,000 new messages arrive in the cytoplasm each minute. As the transcription and processing rates cited above can support such an export rate (i.e. each minute, ~11,000 primary transcripts are made, with ~2,700 being exported), these assumptions are probably broadly correct. Note that we are concerned in the discussion below with reconciling differences of about fivefold.

One obvious possibility is that downstream sites represent individual transcripts that have left transcription sites. A number of reasons make this unlikely. First, our methods would have to be sensitive enough to detect individual transcripts even when they contained very different degrees of substitution with bromine, if most downstream sites are detected (Table 2). Second, even if all unwanted transcripts are completely degraded at transcription sites, we should see 2,700 new downstream sites each minute, and not 600. Third, export of 600 new messages each minute to the cytoplasm is below the 2,000 needed to maintain message levels. As a result, both input from transcription sites and output to the cytoplasm are too low, suggesting that each downstream site must contain ~5 transcripts. If fewer transcripts are completely degraded, or if unwanted transcripts are degraded after export from transcription sites, downstream sites will contain correspondingly more transcripts. (Probably no degradation takes place between transcription and downstream sites; Fig. 3E,F.)

A second possibility equates downstream sites with processing sites; transcripts would leave synthetic sites one at a time to accumulate first in downstream sites, before travelling on to pores; if transfer occurred rapidly enough, individual transcripts would not be detected in transit. Then, we should again see label in 2,700 new downstream sites each minute, and not 600. An unlikely variant invokes some mechanism to direct 2,700 different transcripts to only 600 downstream/splicing sites in the first minute, and then another 2,700 transcripts to another 600 sites in the second, and so on; however, it is difficult to imagine what that mechanism might be.

A third, surprising, possibility is consistent with the data; transcripts would be shipped in groups of ~5, with each shipment being detected as 1 downstream site. Then, ≥2,700 transcripts in ~600 shipments would leave transcription sites each minute, a rate sufficient to maintain message levels in the cytoplasm. This possibility also explains why downstream sites are so homogeneous in size, despite large variations in the length of individual transcripts; if transcripts are partitioned randomly among shipments, those shipments inevitably vary less in size than individual transcripts. It also explains why most downstream sites might be detected, as even an insensitive method becomes sensitive enough when each site contains so many brominated residues. Furthermore, messages may be shipped in groups in the cytoplasm (Ainger et al., 1993; Barbarese et al., 1995; Knowles et al., 1996). A fourth possibility that combines aspects of the second and third is also consistent with the data. Groups of ~5 transcripts could be shipped together to accumulate in (static) downstream/processing sites, before moving on to pores; again, if transfer occurred rapidly enough, transcripts would not be detected in transit. Whether one of the last two possibilities applies will have to await detailed knowledge of the number of transcripts

in downstream sites, and this will probably come from the high-resolution structure of 200 S particles (see below).

### The relationship between downstream sites, SR sites, and 200 S particles

Our results suggest that labelled downstream sites are a subset of the sites that contain SR proteins, and that 200 S particles are derived from these 'SR sites'. 200 S particles are large, tetrameric, particles, for which a low-resolution structure is available, that probably transport mRNA to the pore (for reviews see Yitzhaki et al., 1996, and Sperling et al., 1997). First, downstream sites, SR sites and the particles have roughly similar diameters (i.e. ~77, 83 and 50 nm, respectively). The smaller size of particles can be explained by shrinkage during negative staining (Bozzola and Russell, 1992) and our use of an immunolabelling method that overestimates site diameter (see Results). Second, downstream sites and 200 S particles both contain SR antigens (Fig. 5E). Third, Br-RNA flows into SR sites and 200 S particles with the expected kinetics (Table 5). If each particle contains ~5 transcripts, the RNA-protein ratio would be about one-sixth that found in a ribosome. Then, one structure, the 200 S particle, might accommodate messages with lengths up to five times the average.

We had feared that Br-RNA would not be spliced, and that unspliced RNA might not follow the normal pathway to the cytoplasm. However, the presence of Br-RNA in 200 S particles makes it unlikely that the flow of Br-RNA through 200 S particles is a pathological response to a failure to splice Br-RNA; splicing is disrupted when cells are subjected to a heat shock, but improperly spliced transcripts are nevertheless packaged normally into 200 S particles (Miriami et al., 1994).

### The aberrant accumulation at the pore

Various RNA species have been detected in transit through pores, usually concentrated on one or other side (e.g. Dworetzky and Feldherr, 1988; Amberg et al., 1992; Huang et al., 1994; Fay et al., 1997; Panté et al., 1997). After growth in low concentrations of Br-U, we find little Br-RNA at the periphery (Fig. 1D); however, after growth in high concentrations, Br-RNA backs up at pores, to accumulate within ~400 nm of the membrane (e.g. Table 7). This raises the possibility that natural transcripts are checked when they first dock on to the basket (Davis, 1995; Panté and Aebi, 1996; Daneholt, 1997; Nigg, 1997); if they fail to pass this checkpoint, they might disengage and be degraded. Then, Br-RNA could accumulate here because, being incompletely spliced, it could not pass the checkpoint, and, on rejection, it is more resistant to degradation (Sierakowska et al., 1989).

### A working map of the pathway

A simple map consistent with the data is as follows (Fig. 8). ~75,000 active polymerases are concentrated in ~5,500 extra-nucleolar transcription sites (diameter ~80 nm). We call these sites 'factories', as each contains ~15 active polymerases (Iborra et al., 1996). These factories produce ~11,000 primary transcripts each minute, and they also splice wanted transcripts and degrade unwanted ones (Misteli and Spector, 1997; Steinmetz, 1997). Each minute, ~2,700 wanted transcripts leave the factories in ~600 shipments (diameter ~80 nm), each containing ~5 transcripts and phosphorylated SR proteins detected by monoclonal antibody 104. These complexes can be isolated on sucrose gradients as 200 S particles. At any one time, ~90,000 such shipments are on their way to the pore. These shipments do not normally pass through perichromatin granules (Fig. 1C). They dock at an efficient checkpoint just inside the pore, where wanted messages are quickly allowed through, and rejected messages back up. Usually only ~20% pores are associated with a docked complex, but transcripts containing high levels of bromine create a bottleneck, with a resulting accumulation within 400 nm of the membrane. Unfortunately, our results shed no light on whether molecular 'motors' transport mRNA along 'tracks' to the pore (Lawrence et al., 1989; Rosbash and Singer, 1993; Kramer et al., 1994). However, these high-resolution techniques should enable us to see: (i) if mRNA colocalizes with any known components of such 'motors' or 'tracks', and (ii) which other proteins are associated with RNA in transit (for some candidate proteins, see Dreyfuss et al., 1993; Daneholt, 1997).

Transcription and downstream sites are both marked by clusters of gold particles with diameters of ~80 nm, so the numbers of sites calculated above are based on diameters of 80 nm. However, the true diameters may be smaller as the use of immunogold probes with lengths of ~20 nm long can lead to an overestimate of site diameter (Iborra and Cook, 1998), and isolated SR particles have diameters of ~50 nm (Sperling et al., 1997). Therefore we recalculated the values described above using diameters of 50 nm. Then, a typical nucleus would contain ~8,000 transcription sites and ~140,000 downstream sites; ~2,700 wanted transcripts would leave transcription sites each minute, to generate ~950 new downstream sites with each containing ~3 messages.

We thank the Cancer Research Campaign and the Wellcome Trust for support, Drs M. Hollingshead, E. M. M. Manders, and J. Renau-Piqueras for kindly supplying reagents or software, and A. Pombo, J. Sanderson and J. Bartlett for their help.

### Corrigendum

Active RNA polymerases are localized within discrete transcription 'factories' in human nuclei
by F. J. Iborra, A. Pombo, D. A. Jackson and P. R. Cook (1996) *J. Cell Sci.* **109**, 1427-1436.

In this paper, numbers of transcription sites ('factories') in the three-dimensions of a nucleus were calculated from numbers seen in two-dimensional sections. We apologise for errors made in some calculations concerning samples analyzed by post-embedment labelling and electron microscopy. In Table 1, the measured numbers of clusters per $\mu m^2$ are correct, but calculated numbers of clusters per $\mu m^3$, and the total number of clusters per nucleus, are incorrect. Corrected values for the number of clusters per nucleus are 4,900 (T sites), 5,000 (pol II sites) and 5,600 (pol II sites, unlysed cells). This means that numbers of sites per nucleus ranged from 2,000-5,600 (rather than 2,000-2,700 as originally stated). The central conclusion of the paper - namely that many active polymerases are concentrated in each site - remains unaffected by these corrections.

## REFERENCES


**Ainger, K., Avossa, D., Morgan, F., Hill, S. J., Barry, C., Barbarese, E. and Carson, J. H.** (1993). Transport and localization of exogenous MBP mRNA microinjected into oligodendrocytes. *J. Cell Biol.* **123**, 431-441.

**Alzhanova-Ericsson, A. T., Sun, X., Visa, N., Kiseleva, E., Wurtz, T. and Daneholt, B.** (1996). A protein of the SR family of splicing factors binds extensively to exonic Balbiani ring pre-mRNA and accompanies the RNA from the gene to the nuclear pore. *Genes Dev.* **10**, 2881-2893.

**Amberg, D. C., Goldstein, A. L. and Cole, C. N.** (1992). Isolation and characterization of RAT1: an essential gene of *Saccharomyces cerevisiae* required for the efficient nucleocytoplasmic trafficking of mRNA. *Genes Dev.* **6**, 1173-1189.

**Barbarese, E., Koppel, D. E., Deutscher, M. P., Smith, C. L., Ainger, K., Morgan, F. and Carson, J. H.** (1995). Protein translocation components are colocalized in granules of oligodendrocytes. *J. Cell Sci.* **108**, 2781-2790.

**Bastos, R., Panté, N. and Burke, B.** (1995). Nuclear pore complex proteins. *Int. Rev. Cytol.* **162B**, 257-302.

**Bozzola, J. J. and Russell, L. D.** (1992). *Electron Microscopy: Principles and Techniques for Biologists*. Jones and Bartlett, Boston.

**Buss, F. and Stewart, M.** (1995). Macromolecular interactions in the nucleoporin p62 complex of rat nuclear pores: binding of nucleoporin p54 to the rod domain of p62. *J. Cell Biol.* **128**, 251-261.

**Cáceres, J. F., Misteli, T., Screaton, G. R., Spector, D. L. and Krainer, A. R.** (1997). Role of the modular domains of SR proteins in subnuclear localization and alternative splicing specificity. *J. Cell Biol.* **138**, 225-238.

**Colwill, K., Pawson, T., Andrews, B., Prasad, J., Manley, J. L., Bell, J. C. and Duncan, P. I.** (1996). The Clk/Sty protein kinase phosphorylates SR splicing factors and regulates their intranuclear distribution. *EMBO J.* **15**, 265-275.

**Corbett, A. H. and Silver, P. A.** (1997). Nucleocytoplasmic transport of macromolecules. *Microbiol. Mol. Biol. Rev.* **61**, 193-211.

**Cox, R. F.** (1976). Quantitation of elongating form A and B RNA polymerases in chick oviduct nuclei and effects of estradiol. *Cell* **7**, 455-465.

**Daneholt, B.** (1997). A look at messenger RNP moving through the nuclear pore. *Cell* **88**, 585-588.

**Davis, L. I.** (1995). The nuclear pore complex. *Annu. Rev. Biochem.* **64**, 865-896.

**Dreyfuss, G., Matunis, M. J., Pinol-Roma, S. and Burd, C. G.** (1993). hnRNP proteins and the biogenesis of mRNA. *Annu. Rev. Biochem.* **62**, 289-321.

**Dworetzky, S. I. and Feldherr, C. M.** (1988). Translocation of RNA-coated gold particles through the nuclear pores of oocytes. *J. Cell Biol.* **106**, 575-584.

**Fakan, S., Puvion, E. and Spohr, G.** (1976). Localization and characterization of newly synthesized nuclear RNA in isolated rat hepatocytes. *Exp. Cell Res.* **99**, 155-164.

**Fakan, S.** (1994). Perichromatin fibrils are *in situ* forms of nascent transcripts. *Trends Cell Biol.* **4**, 86-90.

**Fay, F. S., Taneja, K. L., Shenoy, S., Lifshitz, L. and Singer, R. H.** (1997). Quantitative digital analysis of diffuse and concentrated nuclear distributions of nascent transcripts, SC35 and poly(A). *Exp. Cell Res.* **231**, 27-37.

**Griffiths, G.** (1993). *Fine Structure Immunocytochemistry*. Springer-Verlag, Berlin-Heidelberg, 459pp.

**Harris, H. and Watts, J. W.** (1962). The relationship between nuclear and cytoplasmic ribonucleic acid. *Proc. Roy. Soc. Ser. B.* **156**, 109-121.

**Hesketh, J. E. and Pryme, I. F.** (1991). Interaction between mRNA, ribosomes and the cytoskeleton. *Biochem. J.* **277**, 1-10.

**Hozák, P., Hassan, A. B., Jackson, D. A. and Cook, P. R.** (1993). Visualization of replication factories attached to a nucleoskeleton. *Cell* **73**, 361-373.

**Hozák, P., Cook, P. R., Schöfer, C., Mosgöller, W. and Wachtler, F.** (1994). Site of transcription of ribosomal RNA and intra-nucleolar structure in HeLa cells. *J. Cell Sci.* **107**, 639-648.

**Huang, S. and Spector, D. L.** (1991). Nascent pre-mRNA transcripts are associated with nuclear regions enriched in splicing factors. *Genes Dev.* **5**, 2288-2302.

**Huang, S., Deerinck, T. J., Ellisman, M. H and Spector, D. L.** (1994). In vivo analysis of the stability and transport of nuclear poly(A)$^+$ RNA. *J. Cell Biol.* **126**, 877-899.

**Iborra, F. J., Pombo, A., Jackson, D. A. and Cook, P. R.** (1996). Active RNA polymerases are localized within discrete transcription 'factories' in human nuclei. *J. Cell Sci.* **109**, 1427-1436.

**Iborra, F. J. and Cook, P. R.** (1998). The size of sites containing SR proteins in human nuclei: problems associated with characterizing small structures by immunogold labelling. *J. Histochem. Cytochem.* **46** (in press).

**Izaurralde, E. and Mattaj, I. W.** (1995). RNA export. *Cell* **81**, 153-159.

**Jackson, D. A. and Cook, P. R.** (1985). Transcription occurs at a nucleoskeleton. *EMBO J.* **4**, 919-925.

**Jackson, D. A., Hassan, A. B., Errington, R. J. and Cook, P. R.** (1993). Visualization of focal sites of transcription within human nuclei. *EMBO J.* **12**, 1059-1065.

**Jackson, D. A., Iborra, F. J., Manders, E. M. M. and Cook, P. R.** (1998). Numbers and organization of RNA polymerases, nascent transcripts and transcription units in HeLa nuclei. *Mol. Biol. Cell* **9**, 1523-1536.

**Jacobson, A. and Peltz, S. W.** (1996). Interrelationships of the pathways of mRNA decay and translation in eukaryotic cells. *Annu. Rev. Biochem.* **65**, 693-739.

**Knowles, R. B., Sabry, J. H., Martone, M. A., Ellisman, M., Bassell, G. J. and Kosik, K. S.** (1996). Translocation of RNA granules in living neurons. *J. Neurosci.* **16**, 7812-7820.

**Kramer, A.** (1996). The structure and function of proteins involved in mammalian pre-mRNA splicing. *Annu. Rev. Biochem.* **65**, 367-409.

**Kramer, J., Zachar, Z. and Bingham, P. M.** (1994). Nuclear pre-mRNA metabolism: channels and tracks. *Trends Cell Biol.* **4**, 35-37.

**Lasnitzki, I.** (1992). Organ culture. In *Animal Cell Culture: A Practical Approach* (ed. R. I. Freshney), pp. 213-261. IRL Press, Oxford.

**Lawrence, J. B., Singer, R. H. and Marselle, L. M.** (1989). Highly localised tracks of specific transcripts within interphase nuclei visualised by in situ hybridisation. *Cell* **57**, 493-502.

**Lewin, B.** (1974). *Gene Expression-2: Eukaryotic Chromosomes*, vol. II. Wiley, London.

**Miriami, E., Sperling, J. and Sperling, R.** (1994). Heat shock affects 5' splice selection, cleavage and ligation of CAD pre-mRNA in hamster cells, but not its packaging in lnRNP particles. *Nucl. Acids Res.* **22**, 3084-3091.

**Misteli, T. and Spector, D. L.** (1997). Protein phosphorylation and the nuclear organization of pre-mRNA splicing. *Trends Cell Biol.* **7**, 135-138.

**Neugebauer, K. M. and Roth, M. B.** (1997). Distribution of pre-mRNA splicing factors at sites of RNA polymerase II transcription. *Genes Dev.* **11**, 1148-1159.

**Nigg, E. A.** (1997). Nucleocytoplasmic transport: signals, mechanisms and regulation. *Nature* **386**, 779-787.

**Panté, N. and Aebi, U.** (1996). Molecular dissection of the nuclear pore complex. *Crit. Rev. Biochem. Mol. Biol.* **31**, 153-199.

**Panté, N., Jarmolowski, J., Izaurralde, E., Sauder, U., Baschong, W. and Mattaj, I. W.** (1997). Visualizing nuclear export of different classes of RNA by electron microscopy. *RNA* **1**, 498-513.

**Penman, S.** (1995). Rethinking cell structure. *Proc. Nat. Acad. Sci. USA* **92**, 5251-5257.

**Puvion, E. and Puvion-Dutilleul, F.** (1996). Ultrastructure of the nucleus in relation to transcription and splicing: roles of perichromatin fibrils and interchromatin granules. *Exp. Cell Res.* **229**, 217-225.

**Romac, J. M. and Keene, J. D.** (1995). Overexpression of the arginine-rich carboxy-terminal region of U1 snRNP 70K inhibits both splicing and nucleocytoplasmic transport of mRNA. *Genes Dev.* **9**, 1400-1410.

**Rosbash, M. and Singer, R. H.** (1993). RNA travel: tracks from DNA to cytoplasm. *Cell* **75**, 399-401.

**Ross, J.** (1995). mRNA stability in mammalian cells. *Microbiol. Rev.* **59**, 423-450.

**Roth, M. B., Zahler, A. M. and Gall, J. G.** (1990). A monoclonal antibody that recognizes a phosphorylated epitope stains lampbrush chromosomes and small granules in the amphibian germinal vesicle. *J. Cell Biol.* **111**, 2217-2223.

**Schmittgen, T. D., Danenberg, K. D., Horikoshi, T., Lenz, H.-J. and Dannenberg, P. V.** (1994). Effects of 5-fluoro- and 5-bromouracil substitution on the translation of human thymidylate synthase mRNA. *J. Biol. Chem.* **269**, 16269-16275.

**Sharp, P. A.** (1994). Split genes and RNA splicing. *Cell* **77**, 805-815.

**Sierakowska, H., Shuklas, R. R., Dominski, Z. and Kole, R.** (1989). Inhibition of pre-mRNA splicing by 5-fluoro-, 5-chloro-, and 5-bromouridine. *J. Biol. Chem.* **264**, 19185-19191.

**Spector, D. L.** (1993). Macromolecular domains within the cell nucleus. *Annu. Rev. Cell. Biol.* **9**, 265-315.

**Sperling, R., Sperling, J., Levine, A. D., Spann, P., Stark, G. R. and Kornberg, R. D.** (1985). Abundant nuclear ribonucleoprotein form of CAD RNA. *Mol. Cell Biol.* **5**, 569-575.

**Sperling, R., Koster, A. J., Melamed-Bussudo, C., Rubinstein, A., Angenitzki, M., Berkovitch-Yellin, Z. and Sperling, J.** (1997). Three-

dimensional image reconstruction of large nuclear RNP (lnRNP) particles by automated electron tomography. *J. Mol. Biol.* **267**, 570-583.

**Steinmetz, E. J.** (1997). Pre-mRNA processing and the CTD of RNA polymerase II: the tail that wags the dog? *Cell* **89**, 491-494.

**Verheijen, R., van Venrooij, W. and Ramaekers, F.** (1988). The nuclear matrix: structure and composition. *J. Cell Sci.* **90**, 11-36.

**Wansink, D. G., Schul, W., van der Kraan, I., van Steensel, B., van Driel, R. and de Jong, L.** (1993). Fluorescent labelling of nascent RNA reveals transcription by RNA polymerase II in domains scattered throughout the nucleus. *J. Cell Biol.* **122**, 283-293.

**Wansink, D. G., Nelissen, R. L. and de Jong, L.** (1994). In vitro splicing of pre-mRNA containing bromouridine. *Mol. Biol. Rep.* **19**, 109-113.

**Williams, M.** (1977). Quantitative methods in biology. In *Practical Methods in Electron Microscopy,* vol. 6 (ed. A. M. Glauert). North-Holland, Amsterdam.

**Yitzhaki, S., Miriami, E., Sperling, R. and Sperling, J.** (1996). Phosphorylated ser/arg-rich proteins: limiting factors in the assembly of 200S large nuclear ribonucleoprotein particles. *Proc. Nat. Acad. Sci. USA* **93**, 8830-8835.

**Zachar, Z., Kramer, J., Mims, I. K. and Bingham, P. M.** (1993). Evidence for channeled diffusion of pre-mRNAs during nuclear RNA transport in metazoans. *J. Cell Biol.* **121**, 729-742.

**Zahler, A. M., Lane, W. S., Stolk, J. A. and Roth, M. B.** (1992). SR proteins: a conserved family of pre-mRNA splicing factors. *Genes Dev.* **6**, 837-847.